Proceedings of 15th International Marine Design Conference (IMDC-2024)
June 2-6, 2024
Amsterdam, the Netherlands

Comparison and Evaluation of Learning Capabilities of Deep Learning Methods for Predicting Ship Motions

Mingyang Zhang [1,*] , Cong Liu [1], Pentti Kujala [1,2], and Spyros Hirdaris [3]

ABSTRACT

The development of intelligent ship control systems in real-world conditions relies heavily on the accurate identification and prediction of ship seakeeping and maneuvering trajectories. In this study, we comprehensively evaluate a selection of deep learning methods to assess their learning capabilities in terms of idealizing ship motion behavior in realistic operational environments. To recover real conditions, we utilize historical Automatic Identification System (AIS) data and a time domain 6 Degree of Freedom (6-DoF) grounding dynamics model to generate ship motion sequences for a Ro-Ro passenger ship operating in the Gulf of Finland. Via a rigorous evaluation process, we validate the performance of these methods using extensive data streams. The analysis includes the identification and estimation of uncertainties between two ports. The paper demonstrates the proficiency of the selected deep learning methods in capturing ship maneuvering features, their potential use in the design of ship control and intelligent decision support systems.

KEY WORDS

Seakeeping, Maneuvering, Deep learning methods, Design for safety, Ship systems.

INTRODUCTION

Seakeeping prediction methods can enhance our understanding of the dynamic behaviour of ships in stochastic seaways. The models are valuable for improving ship design operational efficiency and safety of ship operations. The development and use of intelligent decision support systems should account for motions and manoeuvres in real operational conditions. Predicting ship motions under real conditions provides a unique opportunity to help crew members understand ship dynamics in advance of a collision or grounding event (Zhang et al., 2023). The integration of empirical data with neural networks in deep learning models shows great promise. However, among the multitude of neural network models, the method that best captures ship manoeuvring features requires comparison and evaluation. Therefore, this paper aims to evaluate the learning capabilities of selected deep learning methods.

With the ongoing advancement in sensor and identification technologies, ship maneuvering system identification methods have emerged as a distinct set of techniques for predicting ship motions. Ship maneuvering parameter identification models are categorized into parametric and non-parametric. Parametric estimation models quantify ship dynamics using established ship theory (e.g., Maneuvering Modelling Group - MMG or Abkowitz models), to train large data sets. Recently the nu- Support Vector Machine (SVM) and a 3-DOF Abkowitz model have been utilized (Wang et al., 2019), while the extended Kalman Filter (EKF) has been coupled with the MMG model (Zeng et al., 2021) to predict hydrodynamic derivatives (Liu et al., 2021). Taimuri et al., (2022) introduced a predictive analytics approach for grounding avoidance using a rapid 6-DoF ship manoeuvring model. However, incorporating hydrometeorological conditions (wave, wind, current, etc.) into these methods poses challenges.

1. Aalto University, Department of Mechanical Engineering, Marine and Arctic Technology Group, Espoo, Finland
2. Tallinn University of Technology, Estonian Maritime Academy, Tallinn, Estonia
3. American Bureau of Shipping - ABS, Athens, Greece
* Corresponding Author: mingyang.0.zhang@aalto.fi

Submitted: 15 February 2024, Revised: 18 April 2024, Accepted: 1 May 2024, Published: 19 May 2024

Conference paper, DOI: https://doi.org/10.59490/imdc.2024.838 e-ISSN: 3050-4864

Non-parametric estimation methods quantify ship dynamics without relying on predefined models. Prominent models include Artificial Neural Networks (ANN) (Silva et al., 2022), machine learning methods, such as Gaussian Process Regression (GPR) (Ouyang et al., 2021; Ramirez et al., 2022), Recurrent Neural Networks (RNN) (D'Agostino et al., 2023), Long Short-Term Memory models (LSTM) (Sun et al., 2022; Zhang et al., 2021), Gated Recurrent Units (GRU) (Zhou et al., 2023), and Transformers (Zhang et al., 2023). These models can be trained using data from simulated free-running tests or sea trials. Recently, Luo et al. developed an ANN model to predict the 3-DOF motion of unmanned surface vehicles (Luo et al., 2022). Non-parametric models have shown potential in identifying ship motion features and rapidly predict ship motions.

To analyze the differences in predicting ship motions using deep learning methods this paper evaluates and compares the learning efficacy and capabilities of the above-mentioned methods.

SHIP MOTIONS AND DATA

The analysis of ship motions often treats the ship as a rigid body moving in six degrees of freedom (6-DOF), using an earth- and ship body-fixed systems. In this paper, to capture the 6-DOF ship motions in real operational conditions, AIS (Automatic Identification System) ship trajectories are reconstructed for a ship operating between two ports. Time-domain hydro-meteorological data are sourced from now-cast data providers, and GEBCO (General Bathymetric Chart of the Oceans). Bathymetry data are employed to map the waterway (see Zhang et al., 2023 and Figure 1).

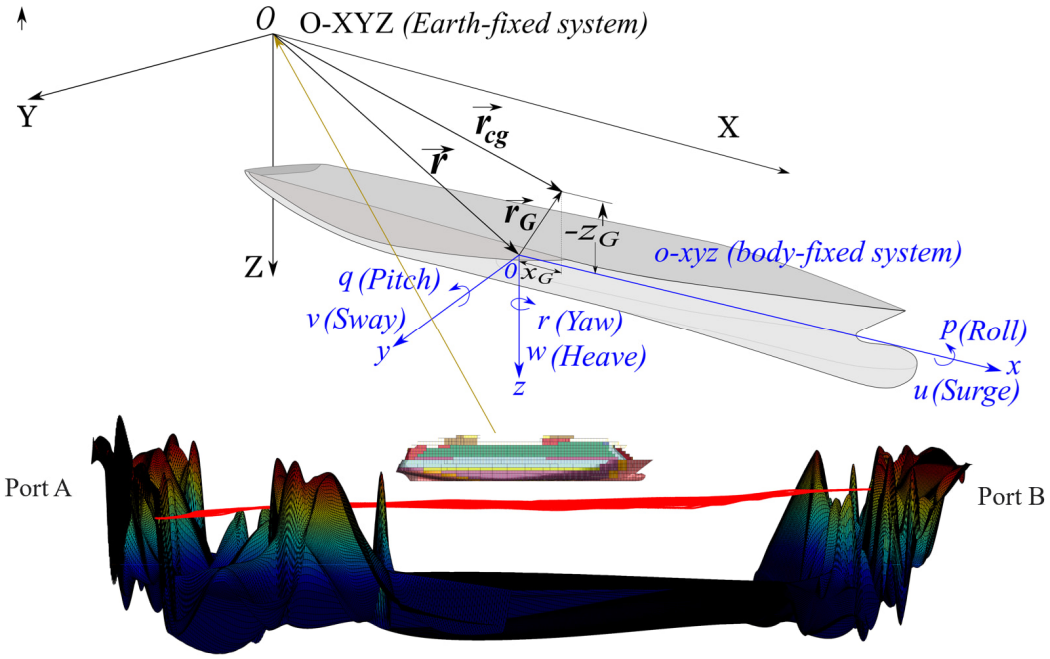

Figure 1: 6-DoF ship motions along ship trajectories between two ports.

The data collected serve as inputs to the FSI model of Taimuri et al., (2022) which idealizes the impact of operational conditions and control devices on ship motions. A Proportional Derivative (PD) controller is utilized to adjust the rudder according to the ship predefined heading, thus autonomously maintaining the desired AIS track for each voyage in real-time, see Zhang et al. (2023). The 6-DOF motions of the ship are depicted in Figure 2. The data utilized to compare and evaluate the learning capabilities of the selected deep learning methods are outlined in Section 3.

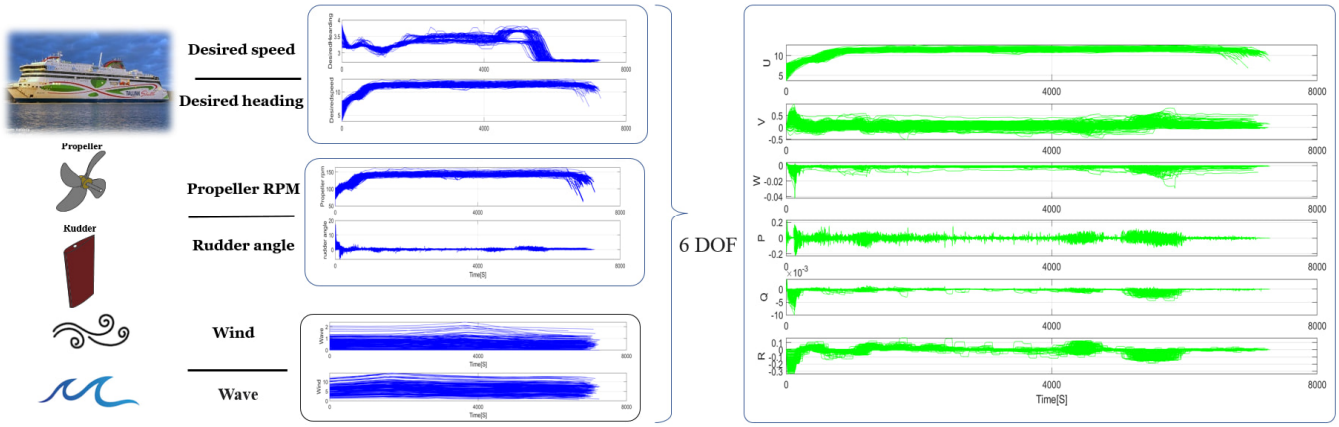

Figure 2: The ship maneuvering commands and the corresponding 6 DOF ship motions

METHODS

This section offers an overview of 6 deep learning methods used for ship motion predictions, illustrating the operating principles of them and briefly describes the underlying mathematical logic of each method. In addition, these models are used to train ship motion prediction models using varying length of training dataset for the evaluation of model learning capabilities, as shown in Figure 3.

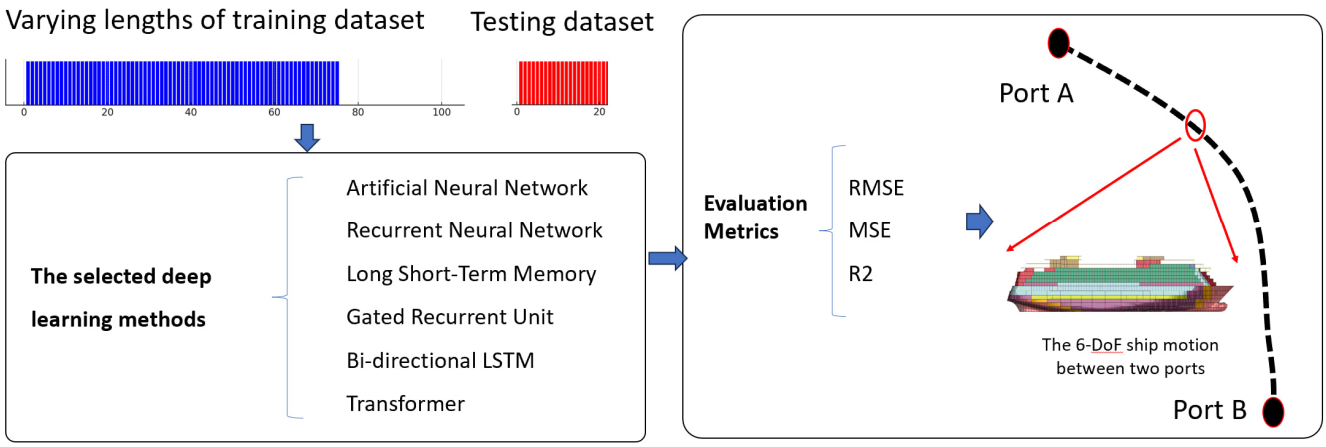

Figure 3: The flowchart of comparison and evaluation of learning capabilities of selected deep learning methods

Selected Deep Learning Models

In this section, the theories behind the 6 deep learning methods (ANN, RNN, LSTM, Bi-LSTM, GRU, and Transformer) used in existing studies are presented to help understand the mathematical logics and the advancements in deep learning technologies for predicting ship motions.

(1) Artificial Neural Networks (ANN)

ANN are a foundational neural network type and a critical component of deep learning technology that may be utilized to predict ship motions (Luo et al., 2022). It comprises of three main layer blocks, namely, an input layer, one or more hidden layers, and an output layer. Each neuron in a layer is connected to every neuron in the preceding and following layers, see Figure 4, where the connections (represented by arrows) contain learnable parameters. The principle of back propagation is employed to adjust the network parameters, by effectively mapping inputs to outputs to approximate various nonlinear functions as follows:

$$h = XW^h + b^h \quad (1)$$
$$y = hW^y + b^y \quad (2)$$

where W^h, W^y are weights and b^h, b^y are biases.

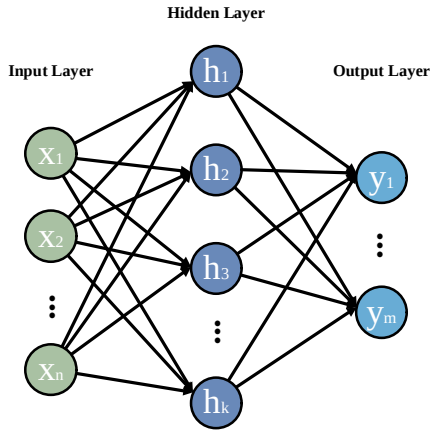

Figure 4: Diagram of ANN architecture

(2) Recurrent Neural Networks (RNN)

RNN represent a type of neural network known for their robust processing of time-series data. Recently, they have been used to predict ship motions (D'Agostino et al., 2023). Unlike ANN, RNN models excel at considering temporal correlations by integrating historical and current information. RNN also serve as a comprehensive framework of neural networks, encompassing various variants, see Figure 5. In a standard RNN, the process begins with an initial hidden state, denoted as H_0. At each time step t, the input X_t is fed into the hidden layer of RNN, where it is combined with the hidden state from the previous time step, see Eq. (3). This combination introduces nonlinearity to the model through an activation function. The activation function, see Figure 5, is typically the hyperbolic tangent - $tanh$. Ultimately, this process results in the generation of the current output and the updated hidden state.

$$H_t = tanh(X_t W_x + H_{t-1} W_h + b_h) \quad (3)$$

where W_x, W_h are the weight matrices and b_h is the bias.

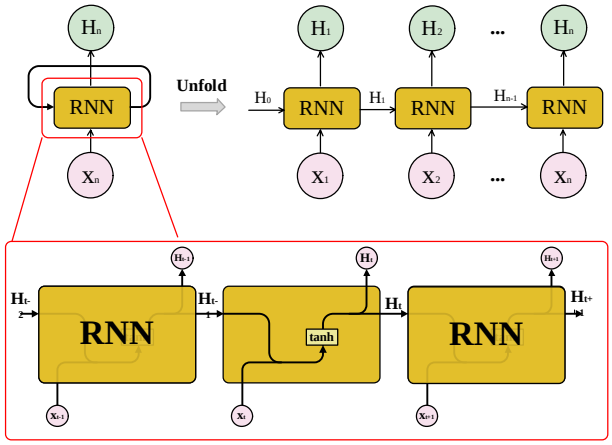

Figure 5: The framework and architecture of RNN

(3) Long Short-Term Memory (LSTM)

In conventional RNN, the issues of gradient explosion and gradient vanishing often arise, hindering a network's ability to predict long sequences effectively (Bianchi et al., 2017). To address this limitation, the LSTM model introduced by Graves, et

al. (2012) was used to train ship motion prediction models (Sun et al., 2022). The LSTM enhances the standard RNN architecture by incorporating three distinct gates namely input, output, and forget gates. These gates allow to selectively retain or discard information, thereby enabling it to effectively utilize long-distance temporal information and significantly improve the model's learning capability.

As illustrated in Figure 6, at a time step t, the current input information is fed into the LSTM, along with the hidden state from the previous time step. This information is then nonlinearly processed by the Sigmoid (σ) activation function to compute the values of the three gates. The computations for these gates are defined as follows:

$$F_t = \sigma(W_F \cdot [H_{t-1}, X_t] + b_F) \quad (4)$$
$$I_t = \sigma(W_I \cdot [H_{t-1}, X_t] + b_I) \quad (5)$$
$$O_t = \sigma(W_O \cdot [H_{t-1}, X_t] + b_O) \quad (6)$$

where W_F, W_I, W_O are the weight matrices of the forget, input and output gates respectively, and b_F, b_I, b_O are the biases of the three gates respectively.

The candidate memory element $\tilde{C}_t$ is calculated as shown in Eq. (7), utilizing the hyperbolic tangent activation function $tanh$. This process determines the information to forget or retain by multiplying the forget gate output F_t with hidden state H_{t-1} at the previous moment. The new cell state C_t is then obtained by adding the memory cell to the information selected by the forget gate. Finally, the latest hidden state H_t is derived by combining the output gate O_t and the new cell state C_t as indicated in Eqs. (8) - (9).

$$\tilde{C}_t = tanh(W_O \cdot [H_{t-1}, X_t] + b_O) \quad (7)$$
$$C_t = F_t * H_{t-1} + I_t * \tilde{C}_t \quad (8)$$
$$H_t = O_t * tanh(C_t) \quad (9)$$

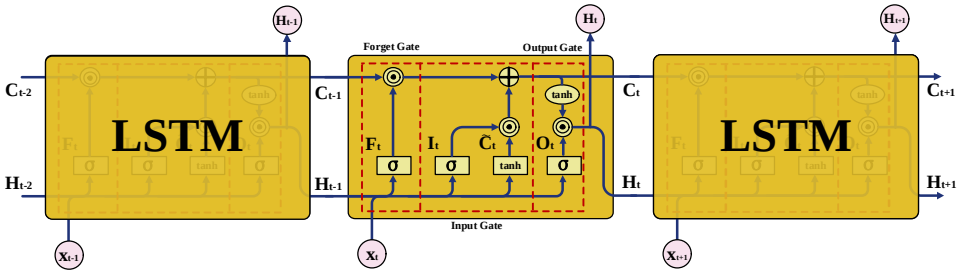

Figure 6: Diagram of LSTM architecture

(4) Gated Recurrent Units (GRU)

GRU are RNN models improved via LSTM and designed to address issues of gradient explosion and vanishing gradients (Chung et al., 2014). Their application for ship motion predictions are presented in Zhou et al. (2023). As compared to LSTM, the GRU simplifies the model architecture by featuring only two gates namely the update gate Z_t and the reset gate R_t, see Figure 7. This streamlined structure allows the GRU to achieve performance comparable to that of LSTM while enhancing training efficiency and computational speed. The computational process of the GRU is outlined as follows:

$$Z_t = \sigma(W_Z \cdot [H_{t-1}, X_t] + b_Z) \quad (10)$$
$$R_t = \sigma(W_R \cdot [H_{t-1}, X_t] + b_R) \quad (11)$$
$$\tilde{H}_t = tanh\,(W_H \cdot [R_t * H_{t-1}, X_t] + b_H) \quad (12)$$
$$H_t = (1 - Z_t) * H_{t-1} + Z_t * \tilde{H}_t \quad (13)$$

where W_Z, W_R, W_H, are weight matrices, b_Z, b_R, b_H are biases, σ is the Sigmoid function, and tanh is the hyperbolic tangent function.

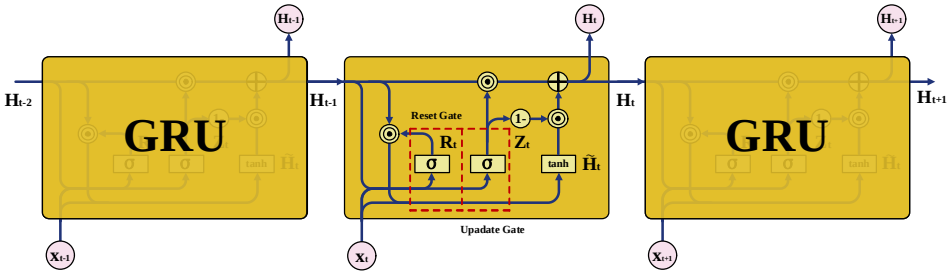

Figure 7: Diagram of GRU architecture

(5) Bi-directional LSTM

In the traditional LSTM model, information can only be recorded from the past, propagating from front to back. However, Bi-directional LSTM (Bi-LSTM) networks are also capable of combining information from both the past and the future (Zhang et al., 2024). This is achieved by constructing associations between the current time step information and the information from both preceding and succeeding time steps, see Figure 8. By leveraging this approach, Bi-LSTM models can learn more complex temporal features, leading to improved prediction accuracy and robustness, see Eqs. (14)-(16).

$$H_t^{fwd} = LSTM_{fwd}(X_t, H_{t-1}^{fwd}) \tag{14}$$

$$H_t^{bwd} = LSTM_{bwd}(X_t, H_{t+1}^{bwd}) \tag{15}$$

$$H_t = [H_t^{fwd}, H_t^{bwd}] \tag{16}$$

where X_t is the input at moment t, H_t^{fwd} is the state of the forward LSTM, H_t^{bwd} is the state of the reverse LSTM, and H_t is the output of the Bi-LSTM after combining the positive and negative states.

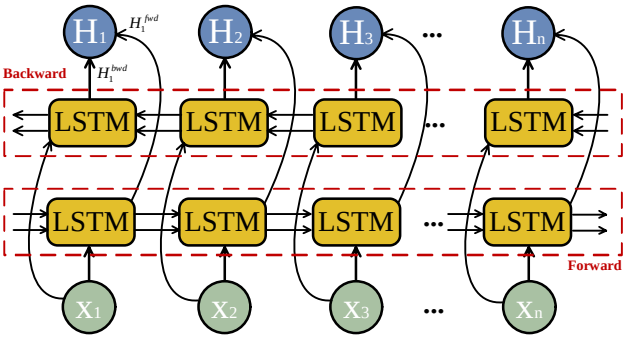

Figure 8: Diagram of Bi-directional LSTM structure

(6) Transformers

The introduction of attention mechanisms has significantly enhanced deep learning methods with widespread application in time series prediction (Zhang et al., 2023). Transformer models employ a multi head self-attention mechanism and an encoder-decoder architecture to extract deep features from training data. Supervised learning trains on historical data, with model parameters updated via back-propagation to progressively approximate true values. The Transformer encoder comprises a series of N identical layers, each containing two sub-layers: a multi-head self-attention mechanism and a fully connected feed-forward network. Both sub-layers undergo normalization operations and incorporate residual connectivity to facilitate information flow. The decoder, similarly, comprises of N identical layers. However, it includes an additional third sub-layer in each sub-layer. This additional sub-layer tasks with masking the self-attention mechanism to ensure predictions for a given position can only depend on previously known outputs, see Figure 9. To incorporate position information within the model, positional encoding is applied at the base of both encoder and decoder layers as follows:

$$PE_{(pos,2i)} = sin(pos/10000^{2i/d_{\text{model}}}) \tag{17}$$

$$PE_{(pos,2i+1)} = cos(pos/10000^{2i/d_{\text{model}}}) \tag{18}$$

where pos is the position and i is the dimension of the d_{model}.

The attention mechanism utilized in the Transformer model is the scaled dot-product attention. This mechanism involves stitching together multiple attention heads to form distinct subspaces, enabling the model to learn features from various perspectives. Additionally, each layer includes a fully connected feed-forward neural network. This network is independent and applied to each position identically across the sublayers. The computation within this network proceeds through the ReLU (Rectified Linear Unit) activation function, as follows:

$$Attention(Q,K,V) = softmax(\frac{QK^T}{\sqrt{d_k}})V \tag{19}$$

$$MultiHead(Q,K,V) = Concat(head_1,\dots,head_h)W^O \tag{20}$$

$$\text{where head}_i = Attention(QW_i^Q, KW_i^K, VW_i^V) \tag{21}$$

$$FFN(x) = max(0, xW_1 + b_1)W_2 + b_2 \tag{22}$$

$$ReLU(x) = (x)^+ = max(0,x) = \begin{cases} x & if x > 0 \\ 0 & if x \leqslant 0 \end{cases} \tag{23}$$

Where Q, K, V are query, key, and value respectively, $\sqrt{d_k}$ is the vector dimension, h is the number of parallel attention heads, W_i^Q, W_i^K, W_i^V are the weight matrices, W_1, W_2 are the weights, and b_1, b_2 are the biases.

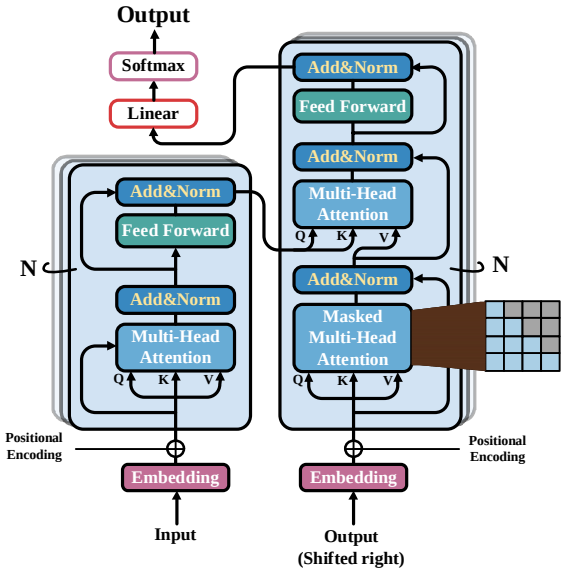

Figure 9: Diagram of Transformer architecture

Model Evaluation Metrics

To evaluate the performance of these selected deep learning models and quantify the errors between the real and the predicted ship motions, Root Mean Square Error (RMSE), Mean Square Error (MSE), and R^2 value (coefficient of determination) were evaluated, as:

$$RMSE = \sqrt{\frac{1}{N}\sum_{n=1}^{N}(y_n - \hat{y}_n)^2} \tag{24}$$

$$MSE = \frac{1}{N}\sum_{n=1}^{N}(y_n - \hat{y}_n)^2 \tag{25}$$

$$R^2 = 1 - \sum_{n=1}^{N}(y_n - \hat{y}_n)^2 / \sum_{n=1}^{N}(y_n - \bar{y}_n)^2 \tag{26}$$

In the above expressions, y_n is the actual value, $\hat{y}_n$ denotes the predicted value, $\bar{y}_n$ is the mean value.

RESULTS AND DISCUSSION

The results presented utilise 400 (80%) of the 500 ship trajectories from Section 2. A 6 DOF ship motions model of each ship trajectory is used to train the selected 6 deep learning models presented in Section 3.1. The remaining 100 (20%) ship trajectories serve for validation purposes. (See Section 4.1). To keep the hyperparameters of these deep learning models unchanged, training sessions encompassing different data volumes are used to examine how the amount of data influences model efficacy, see Section 4.2. Through this comprehensive analysis, attempts to pinpoint the predictive accuracy of models and identify the data volume necessary to achieve training saturation. In this sense the results presented may be useful to develop ship motion prediction models that possess the ability to learn and adapt.

Results of Ship Motions Prediction Using Various Deep Learning Models

Based on the data presented in Section 2, different machine learning models have been utilized to train predictors for ship motions. The inputs to these models are propeller RPM and rudder angle. The outputs are the 6 DOF of ship motions along ship trajectories. Their configurations are outlined in Table 1. Hyperparameters are optimized using a grid search method, with the best parameters determined by the lowest MSE obtained during validation (Zhang et al., 2024).

Table 1: The characteristics of the selected models and the optimal hyperparameters

Model	ANN	RNN	LSTM	Bi-LSTM	GRU	Transformer
Data	2 input variables and 6 output variables					
Architecture	3 layers; 64 hidden units per layer; Early stopping: Patience=10; Optimizer: Adam; Dropout rate: 0.2; Regularization param: 0.1					Encoder: 6 Decoder: 6
Leaning rate	0.001	0.001	0.001	0.001	0.001	Batch Size: 8
Epochs	18	32	17	21	28	Epochs: 48
Batch size	10	15	5	10	10	Inner layers: 1,024

The training and validation losses were calculated based on the basis of training 80% and 20% of 500 ship trajectories, respectively. Table 2 showcases the validation losses for various models, illustrating that the Transformer model exhibits a stronger capability for handling the degrees of freedom in ship motions as compared to models like ANN, RNN, LSTM, GRU, and Bi-LSTM. Theoretically, a Transformer model's advantage stems from its extensive parameter scale, which enhances its predictive performance and learning capabilities. It is also possible that the observed superiority of the Transformer model is partly due to the relatively simplistic complexity settings of the ANN, RNN, LSTM, GRU, and Bi-LSTM models.

Table 2: The performance evaluation on the teasing dataset of the selected ship models

	ANN	RNN	LSTM	Bi-LSTM	GRU	Transformer
RMSE	0.096	0.098	0.067	0.055	0.042	0.022
R^2	0.365	0.375	0.487	0.511	0.574	0.837

To further assess these models, propeller RPM and rudder angle, were chosen to evaluate the generalization capabilities of the trained models. The results indicate that the trained deep learning models are proficient in capturing the characteristics of ship maneuvering under real conditions. However, their accuracy varies. This difference is observed not only in the overall accuracy of the models but also in the prediction accuracy for various motions (Surge, Sway, Heave, Roll, Pitch, Yaw), see Figure 10. Overall, the results indicate that the Transformer model is more effective in capturing nonlinear ship motions that mirror actual operational conditions. This also suggests that its learning capabilities are superior for predicting ship motions in real conditions, as compared to selected deep learning methods.

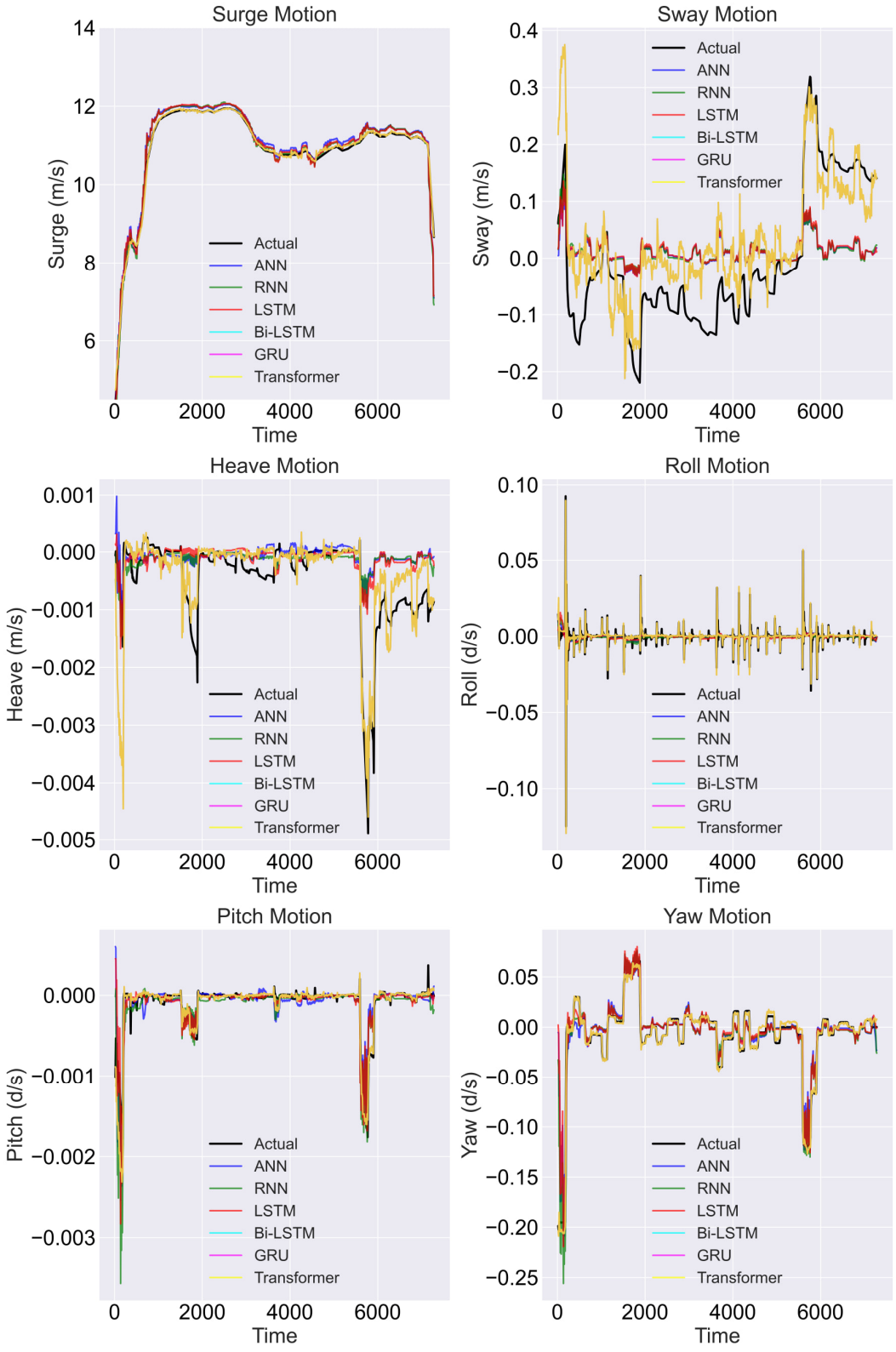

Figure 10: The results of the prediction of ship motion dynamics using different models

Evaluation of Learning Capacities

In Section 4.1, this paper trains and predicts the 6 DOF ship motions using the selected deep learning models. Subsequently, the paper explores how much data is required to saturate results, i.e., to the point where increasing the amount of data no longer

reduces the accuracy. Initially, 400 ship trajectories have been divided into 20 datasets, with the first dataset containing the first 20 trajectories, the second set containing the first 40 trajectories, and so on, until the 20th dataset, which includes all 400 trajectories. An additional 100 trajectories have been reserved as a fixed testing dataset, see Figure 3. The selected deep learning models have been trained, keeping the hyperparameters from Section 4.1 unchanged. This allowed for the incremental increase in the amount of training data against the same testing set and the calculation of test loss, thereby identifying the data volume at which model training reaches saturation.

The test error curves for the various models have been plotted based on the given data with different lengths, see Figure 11. Each line represents the change in error as the lengths of training dataset increases, which could represent iterations in training ship motion predictors using the selected models. It displays the general trend that as the number of ship trajectories increases, the testing loss for each model decreases. This indicates an improvement in the prediction accuracy of these models with the increase of the training database. Figure 11 illustrates that upon reaching saturation, the loss error of these models ranges from 0.4e-3 to 12.5e-3. Among them, the transformer model exhibits the highest accuracy, while the RNN model performs the poorest, with its error being threefold higher than that of the transformer. The losses of LSTM, Bi-LSTM, and GRU are between them.

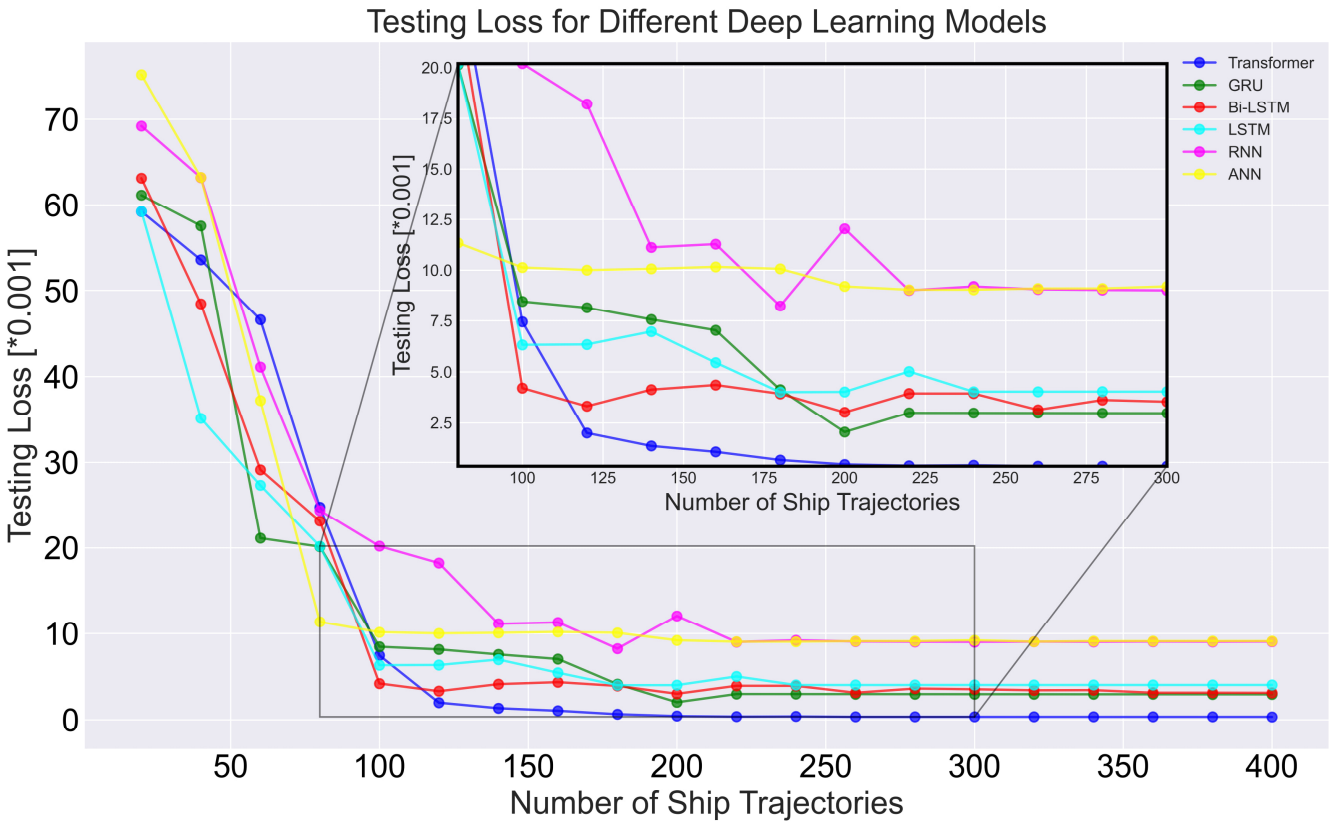

Figure 11: The influences of different lengths of training data on testing loss evaluation

Figure 12 illustrates the data volume thresholds at which various deep learning models reach saturation, demonstrating that each model requires a different dataset size to achieve optimal performance. For instance, the Transformer model reaches peak efficiency at a data volume of 280, while the RNN model achieves its best performance with a data volume of 140, and the ANN requires only 80. Overall, as the training dataset expands, the increase in predictive accuracy halts, indicating that the models have reached their maximum learning capabilities. The ANN and LSTM models appear to plateau earlier than others. This suggests that they require less data to reach their performance limits. It is noted that reaching performance limits does not imply that these models have attained the highest prediction accuracy for ship motions. It merely indicates that the deep learning model may not process additional data to further enhance the model's prediction ability to capture ship motion characteristics.

Other models continue to show improvements with additional data before reaching a plateau. Notably, when data is scarce, the Transformer exhibits the highest accuracy, implying that it has superior learning ability compared to the others and is more adept at capturing the nonlinear movements of ships influenced by hydrological and meteorological conditions. An RNN model requires a substantial amount of data to train effectively, and even then, their accuracy may not be sufficient.

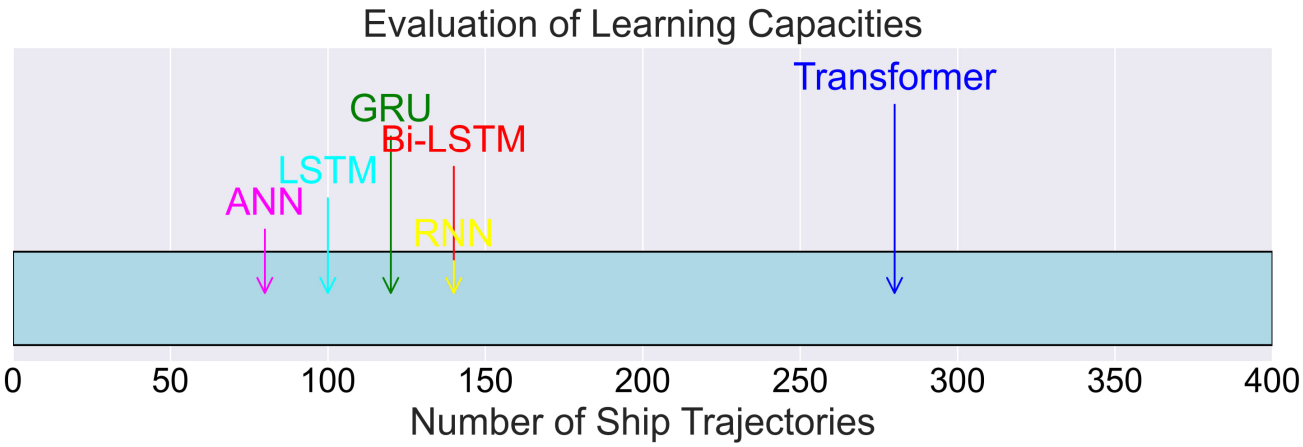

Figure 12: The learning capacities of the selected deep learning model

In predicting nonlinear ship motions, the Transformer model excels due to its remarkable accuracy, especially when dealing with complex dependencies over long sequence in the time domain. However, this model requires substantial computational power and a large volume of training data. Bi-LSTM and GRU models provide a compromise, handling sequences with moderate complexity more efficiently and using fewer resources while maintaining dependable accuracy. On the other hand, traditional ANNs and RNNs are quicker but faultier. The intricacies involved in predicting nonlinear ship motions, render them less effective for sophisticated tasks.

Figure 10 highlights the diverse proficiencies of various models in capturing the six degrees of freedom (6 DOF) of ship motions in the time domain. The Transformer model significantly outperforms others in predicting sway motion. However, for roll and surge predictions, other models also exhibit high accuracy and require less data. There is potential for future research to explore combining two or more models to predict each motion separately. Such hybrid approaches could enhance the precision of predictions by leveraging the strengths of diverse modelling techniques.

CONCLUSIONS

The paper presents a framework for the comparison and evaluation of learning capabilities of the selected deep learning methods that could be used for the prediction of ship motions. To validate the framework, six existing deep learning methods for ship motion predictions are selected, namely ANN, RNN, LSTM, Bi-LSTM, GRU, and Transformer. The models are used to train 6 DOF ship motions predictors displaying the influence of nonlinear effects by using the same data streams along ship trajectories between two ports. It is concluded that their level of accuracy varies (see Table 2 and Figure 11). The paper also evaluates the learning capacities of these selected models in analyzing the impact of data volumes on their effectiveness by utilizing datasets of varying lengths. Generally speaking, the transformer model stands out in terms of accuracy.

In the future, results of this comparison and evaluation of the selected deep learning models may assist in selecting appropriate models for the development of online ship motion prediction tools with adaptive learning capabilities. Such tools are a crucial component of intelligent navigational decision-making systems.

CONTRIBUTION STATEMENT

Mingyang Zhang: Conceptualization; data curation, methodology; writing – original draft. **Cong Liu:** methodology; writing – original draft; writing – review and editing. **Pentti Kujala**: conceptualization; writing – review and editing. **Spyros Hirdaris**: conceptualization; supervision; writing – review and editing.

ACKNOWLEDGEMENTS

The authors express gratitude for the financial support provided by the "RETROFIT solutions to achieve 55% GHG reduction by 2030 (RETROFIT55) – Project No.: 101096068," funded under the Horizons Europe project, as well as by Merenkulun Säätiö. They also extend special thanks to CSC Finland for offering access to their parallel computing facilities. It is important to note that the opinions and findings presented in this paper represent those of the authors alone and may not coincide with the positions of their funding bodies.

REFERENCES

Bianchi, F. M., Maiorino, E., Kampffmeyer, M. C., Rizzi, A., Jenssen, R., Bianchi, F. M., ... & Jenssen, R. (2017). Properties and training in recurrent neural networks. Recurrent Neural Networks for Short-Term Load Forecasting: An Overview and Comparative Analysis, 9-21.

D'Agostino, D., Serani, A., Stern, F., & Diez, M. (2021). Recurrent-type neural networks for real-time short-term prediction of ship motions in high sea state. arXiv preprint arXiv:2105.13102.

Graves, A., & Graves, A. (2012). Long short-term memory. Supervised sequence labelling with recurrent neural networks, 37-45.

Liu, Z., Wu, Z., Zheng, Z., Wang, X., & Soares, C. G. (2021). Modelling dynamic maritime traffic complexity with radial distribution functions. Ocean Engineering, 241, 109990.

Lou, J., Wang, H., Wang, J., Cai, Q., & Yi, H. (2022). Deep learning method for 3-DOF motion prediction of unmanned surface vehicles based on real sea maneuverability test. Ocean Engineering, 250, 111015.

Ouyang, Z. L., & Zou, Z. J. (2021). Nonparametric modeling of ship maneuvering motion based on Gaussian process regression optimized by genetic algorithm. Ocean Engineering, 238, 109699.

Ramirez, W. A., Leong, Z. Q., Nguyen, H., & Jayasinghe, S. G. (2018). Non-parametric dynamic system identification of ships using multi-output Gaussian Processes. Ocean Engineering, 166, 26-36.

Silva, K. M., & Maki, K. J. (2022). Data-Driven system identification of 6-DoF ship motion in waves with neural networks. Applied Ocean Research, 125, 103222.

Sivaraj, S., Rajendran, S., & Prasad, L. P. (2022). Data driven control based on Deep Q-Network algorithm for heading control and path following of a ship in calm water and waves. Ocean Engineering, 259, 111802.

Sun, Q., Tang, Z., Gao, J., & Zhang, G. (2022). Short-term ship motion attitude prediction based on LSTM and GPR. Applied Ocean Research, 118, 102927.

Taimuri, G., Zhang, M., & Hirdaris S. (2022). A Predictive Analytics Method for the Avoidance of Ship Grounding in Real Operational Conditions. SNAME Maritime Convention 2022 26-29 September, Houston, TX, 2022, p. 18.

Wang, Z., Zou, Z., & Soares, C. G. (2019). Identification of ship manoeuvring motion based on nu-support vector machine. Ocean Engineering, 183, 270-281.

Woo, J., Yu, C., & Kim, N. (2019). Deep reinforcement learning-based controller for path following of an unmanned surface vehicle. Ocean Engineering, 183, 155-166.

Zeng, D., Xia, G., & Cai, C. (2021, October). Parameter Identification of Hydrodynamic Model of Ship Using EKF. In 2021 China Automation Congress (CAC) (pp. 1427-1432). IEEE.

Zhang, M., Kujala, P., Musharraf, M., Zhang, J., & Hirdaris, S. (2023). A machine learning method for the prediction of ship motion trajectories in real operational conditions. Ocean Engineering, 283, 114905.

Zhang, M., Taimuri, G., Zhang, J., Hirdaris S. (2022 d). A deep learning method for the prediction of 6-DOF ship motion in real conditions. Proceedings of the Institution of Mechanical Engineers, Part M: Journal of Engineering for the Maritime Environment, Doi 14750902231157852.

Zhang, M., Tsoulakos, N., Kujala, P., & Hirdaris, S. (2024). A deep learning method for the prediction of ship fuel consumption in real operational conditions. Engineering Applications of Artificial Intelligence, 130, 107425.

Zhang, T., Zheng, X. Q., & Liu, M. X. (2021). Multiscale attention-based LSTM for ship motion prediction. Ocean Engineering, 230, 109066.

Zhou, T., Yang, X., Ren, H., Li, C., & Han, J. (2023). The prediction of ship motion attitude in seaway based on BSO-VMD-GRU combination model. Ocean Engineering, 288, 115977.